Int J Thermophys (2007) 28:2028–2040
DOI 10.1007/s10765-007-0297-5

A Study of the Metal Carbide-Carbon Peritectic Phase Transition for the Cr-C System

Y. Yamada · Y. Wang · W. Zheng · N. Sasajima

Published online: 23 October 2007

Abstract The authors recently reported the very first radiometric plateau observation of high-temperature fixed points of metal-carbide carbon peritectics. These act in a similar way to the metal (carbide)-carbon eutectic points in the sense that they can be used at high temperature without being contaminated by their graphite crucibles. The performance seems similar in terms of repeatability and plateau shape. The peritectic transition temperatures are close to the transition temperatures of some of the metal (carbide)-carbon eutectics. In this article, results of further study to understand the melting and freezing involved in these fixed points are reported, with the focus on the Cr_3C_2-C peritectic point. Difficulty in producing an ingot without voids was encountered. To overcome this, a filling technique that takes advantage of the capillary effect was devised. Plateau shapes and microstructures observed with electron-probe microanalysis (EPMA) and back-scattered electron imaging (BSE) for various filling methods were compared. The observation of two fixed-point plateaux, one at the Cr_3C_2-C peritectic point and the other at a lower temperature of the Cr_7C_3-Cr_3C_2 eutectic point, correlates to the presence of two kinds of domains in the observed microstructure. The graphite crucible is shown to play an essential role in realizing peritectic plateaux of good quality.

Keywords Chromium carbide · Eutectic · Fixed point · High temperatures · Peritectic · Radiation thermometry · Temperature standards

Y. Yamada (✉) · Y. Wang · N. Sasajima
Radiation Thermometry Section, Temperature and Humidity Division, National Metrology Institute of Japan, AIST, AIST Tsukuba Central 3-1, 1-1-1 Umezono, Tsukuba, Ibaraki 305-8563, Japan
e-mail: y.yamada@aist.go.jp

W. Zheng
National Institute of Metrology, 18 Beisanhuan Dong Lu, Beijing 100013, China

1 Introduction

High-temperature fixed points are currently the subject of an international project aimed at replacing the high-temperature part of the international temperature scale by a scale mediated by these points [1]. This project focuses on the metal-carbon and metal carbide-carbon (M(C)-C) eutectic fixed points [2], most of which have so far proven to be capable of achieving the required performances.

Recently, some of the authors have reported new high-temperature fixed points located near the temperatures of some of the M(C)-C eutectic fixed points. These are the metal carbide-carbon (MC-C) peritectic points of Mn_7C_3-C (1331°C), Cr_3C_2-C (1826°C), and WC-C (2749°C). In a preliminary investigation, reproducibility of 0.02 K and a melting range of 0.1 K were reported [3], which is of the same quality as the best M-C eutectics reported so far. The reported performance is surprising, if one considers the nature of the peritectic reaction, which involves formation of a nonuniform structure through a slow solidification process that requires diffusion of carbon through the solid carbide phase.

In [3], the cells were prepared from a metal and graphite powder mixture at the carbide composition (except for Mn, for which the mixture was made to be slightly richer in graphite), and were sintered prior to melting to produce a porous ingot structure that retains the structure and shape without flowing after melting.

The Mn_7C_3-C cell was found to break after a few days when exposed to air at room temperature. Rapid oxidation of the metal caused the ingot to expand, thereby breaking the outer wall of the graphite crucible. Why the carbide ingot reacts so rapidly as compared to a pure Mn ingot remains unexplained. However, since the temperature of the Mn_7C_3-C peritectic point almost coincides with the Co-C eutectic point (1324°C), which is already established as a high-temperature fixed point, we decided to focus our investigations on the other two peritectic fixed points.

The current work aims to gain better understanding of the peritectic reaction involved. We report results of an experimental investigation on the Cr_3C_2-C peritectic point, where we study the measured melting and freezing plateaux in conjunction with the microstructures involved. In an accompanying article, we report on the evaluation of the performance of this system as a fixed point [4]. In another article in these proceedings, the WC-C peritectic point is discussed in detail [5].

2 Metal Carbide-Carbon Peritectic Reaction

In Fig. 1, a binary alloy phase diagram is shown for the Cr-C system. At the peritectic point, indicated by (A) in the figure, the solid carbide phase of Cr_3C_2 is in equilibrium with two phases, the liquid phase metal-carbon solution at the 37% carbon atomic composition and the solid graphite phase. The MC-C peritectic reaction and the M(C)-C eutectic reaction can be described as follows, where the transition from left to right corresponds to melting, and the opposite direction to freezing.

<MC-C peritectic reaction>

Solid MC $\longleftrightarrow$ Solid C + Liquid M-C solution

<M(C)-C eutectic reaction>
Solid M(C) + Solid C ⟷ Liquid M-C solution

The two reactions are similar in that the same three types of phases are involved. As the crucible material is a component of the reaction, the feature of inherently contamination-free fixed-point realization in a graphite crucible is maintained in the MC-C peritectic system as in the M(C)-C eutectic points. Therefore, a reproducible melting plateau can be obtained.

However, there are noticeable differences in the two reactions. During a eutectic freezing, the liquid metal-carbon solution separates at the freezing front to form metal (or metal-carbide) and graphite, which attach to the two corresponding solid phases: the diffusion occurs in the liquid phase. In contrast, during a peritectic freezing, the liquid metal-carbon solution initially reacts with the graphite phase with which it has contact and the carbide phase is formed where the reaction occurs, i.e., at the surface of the graphite. When the surface of the graphite becomes totally enveloped by the carbide, carbon must diffuse through the carbide layer to reach the liquid for the reaction to continue: the diffusion occurs in the solid phase.

During a eutectic freezing, the freeze rate is proportional to the heat flux, determined by the difference between the freezing temperature of the fixed point and the temperature of the furnace. During a peritectic freezing, the freeze rate is limited by the speed of diffusion through the solid metal carbide layer which becomes thicker as the freeze progresses. The existence of a second freezing plateau below the peritectic freezing plateau [3] is proof that freezing occurs at the eutectic point between the two carbides Cr_7C_3 and Cr_3C_2 (corresponding to point (B) in Fig. 1), indicating that the peritectic freeze was incomplete and liquid phase remained during further cooling.

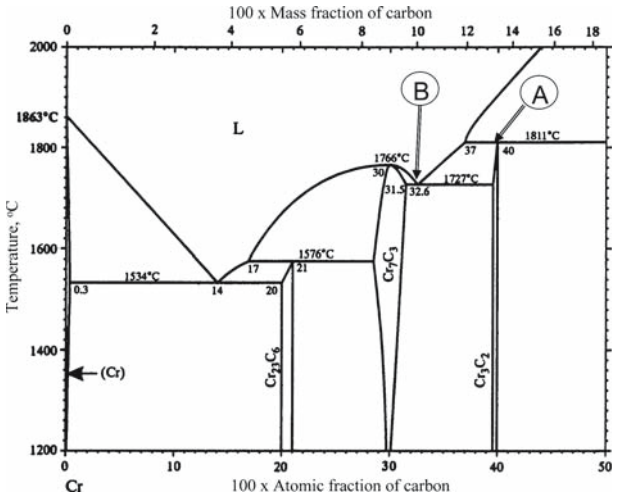

Fig. 1 Cr-C binary phase diagram (original diagram taken from [6])

3 Establishing Fabrication Techniques of MC-C Peritectic Cells

Three types of cell filling methods are compared in this investigation. The cells have the same crucible design as the one shown schematically in [7], with an outer dimension of 24 mm and incorporating a 3-mm-aperture blackbody cavity with an estimated effective emissivity of 0.9996. The graphite crucibles were purified by the manufacturer after machining to better than 99.9995% purity. The metal-graphite powder mixtures all used graphite powder of 99.9999% (supplier: Johnson & Matthey). The powder mixtures were melted in a vertical furnace (manufactured by Nagano, Model VR20-A10) [8].

3.1 Porous Ingot Cell

In the previous investigation [3], the cell was filled to form a porous ingot. For this, chromium powder was mixed with the graphite powder at the Cr_3C_2 carbide composition of 40% atomic fraction of carbon. No inner sleeve or C/C sheet (described below) was applied. The crucible was filled with the powder mixture, and was placed in the vertical furnace, which was then evacuated and flushed with argon. Subsequently, the furnace was heated above the Cr_7C_3–Cr_3C_2 eutectic point of around 1727°C in vacuum and brought down to room temperature for inspection. The ingot appeared to be in a sintered state. The cell was placed back in the furnace and was heated in vacuum this time to above the peritectic melting temperature to melt and form the porous ingot. During this process, contamination of the furnace by chromium due to its high vapor pressure was detected. Therefore, all subsequent fillings were done in Ar.

3.2 Non-porous Ingot Cell

Subsequent attempts to fabricate cells of porous ingot structure from different chromium powder quality or form did not succeed. It was suspected that the powder grain size had to be fine enough for this method to succeed. Although it was not clear why certain powder forms succeed while the others do not, the sintering approach was clearly unreliable, and therefore a non-porous ingot cell was fabricated and its performance was evaluated.

For the non-porous cell, initially the technique that applies C/C sheet around the ingot to prevent breakage was attempted [9]. In this method, the crucible outer wall and the ingot are separated by one or two layers of a 0.5 mm thick purified graphite cloth material (“C/C sheet” TCC-019, manufactured by Toyo Tanso Co. Ltd, with impurity content less than 10 ppm). This acts as a buffer for mechanical stress. However, unlike other metals in the M(C)-C eutectic systems, the C/C sheet absorbed the molten chromium metal and did not function as a buffer layer. The metal, instead, tends to wet and spread along the graphite inner surface of the crucible. This is indicative of the low surface energy of the molten chromium carbon mixture. We therefore applied the conventional filling procedure without the C/C sheet. Attempts to apply a funnel to the crucible to increase the efficiency failed as well: the metal did not flow down into the crucible, due to its high viscosity. Finally, filling was possible by repeatedly

melting small amounts of powder at a time. However, it was found that large voids were present in the ingot. The low surface energy is related to good wetting which makes the molten chromium adhere and spread along the graphite side wall, while its high viscosity prevents it from flowing to the crucible bottom.

3.3 Non-porous Ingot Cell with C/C-Sheet Wick

A new filling method was devised to overcome the formation of the voids. Firstly, layers of C/C sheet were packed tightly in the bottom section of the crucible, spirally around the cavity. Then, the powder mixture of chromium and graphite was placed on top. The amount of chromium was adjusted so that the volume of the molten metal would fill the space occupied by the C/C sheets. The mixture composition was adjusted so that the atomic composition would become 40%, the composition of Cr_3C_2 carbide, when the C/C sheet is totally dissolved in the metal. Then the cell was placed in the vertical furnace to melt. The C/C sheet in this case is employed as a wick so that the molten metal penetrates every corner of the crucible through the capillary effect, and then is dissolved to achieve the required composition. The filling process consists of repetition of this step, by adding C/C-sheet layers on top of the formed ingot section and then the powder mixture above in proportion, each step resulting in a dense filling of the space originally occupied by the C/C-sheet layers. Thus, formation of voids can be prevented. Complete filling was achieved in five repetitions.

In Fig. 2, cross-section photos of test cells are shown. The layers of C/C sheet were placed, in this case, flat on the bottom of a cup-shaped graphite crucible, the metal-graphite powder mixture was filled to the rim, and the crucible heated in a furnace to above the peritectic point. The metal ingot is seen to have exactly replaced the C/C sheet, retaining the rectangular cross-section shape, with hardly any voids. A reference cell is shown, where no C/C sheets were used, and the carbon composition of the mixture is 40%. The ingot in this case was poorly formed, attaching itself to the wall instead of flowing to the bottom.

In Fig. 3, X-ray transmission photos are shown for a Cr_3C_2-C cell filled with and without the C/C sheet. Numerous voids are seen in the cell without the C/C-sheet absorber, in contrast to the cell densely filled with the C/C-sheet absorber. However, a large gap is seen between the second and third ingot sections, showing that further improvement in the filling technique with the C/C-sheet absorber is necessary.

4 Plateau Observations

4.1 Measured Cells and Measurement Setup

Four cells are compared in the current investigation: one porous cell (6SS-1) is measured, which is the same cell as used in the previous investigation [3]. This was prepared from chromium powder of 99.9% nominal purity (supplier: Kojundo Chemical Laboratories Co., Ltd). Two non-porous ingot cells without the C/C-sheet absorber were prepared. One (6SS-2) was prepared from chromium powder from the same lot as used in 6SS-1. The other (6SS-6) used chromium flakes of 99.995% nominal purity

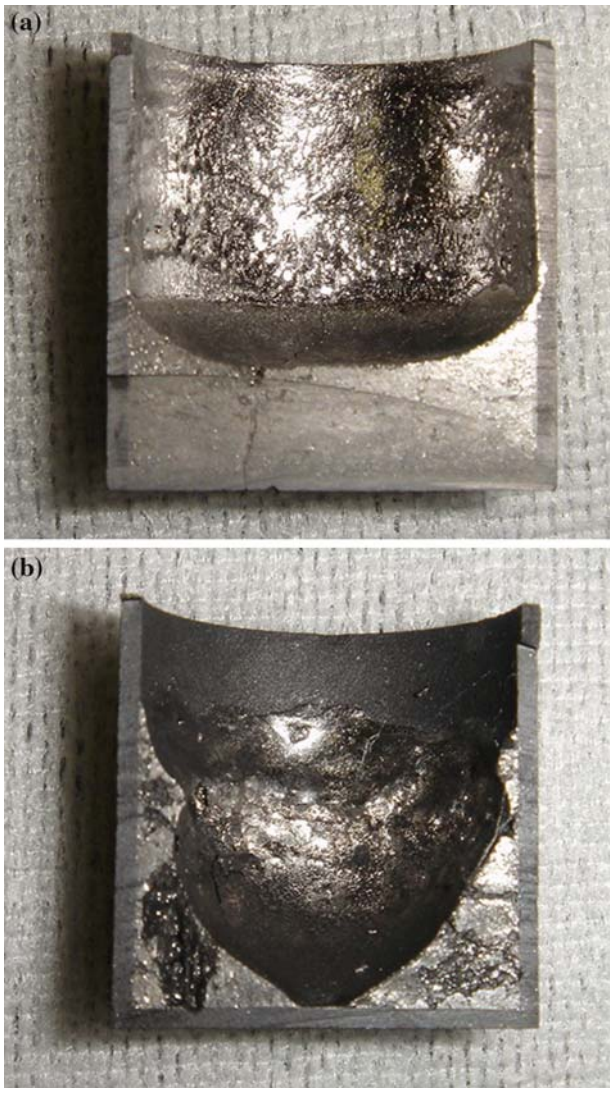

Fig. 2 Test cells for filling with C/C absorber: (**a**) with C/C-sheet absorber and (**b**) without C/C-sheet absorber

(supplier Nikko Metals Co., Ltd). The fourth cell was a non-porous ingot cell utilizing C/C-sheet absorber (6ST-3) prepared from the same chromium flake.

The ingot masses were 11.3, 18.9, 18.2, and 18.2 g, and the apparent densities, calculated from the crucible volume and the ingot mass, were 1.9, 4.5, 4.4, and 4.4 $g \cdot cm^{-3}$ respectively, for 6SS-1, -2, -6, and 6ST-3.

The cells were placed in high-temperature horizontal furnaces and the melting and freezing plateaux were observed by means of two radiation thermometers. These were not calibrated for the measurements; the temperature values have an uncertainty

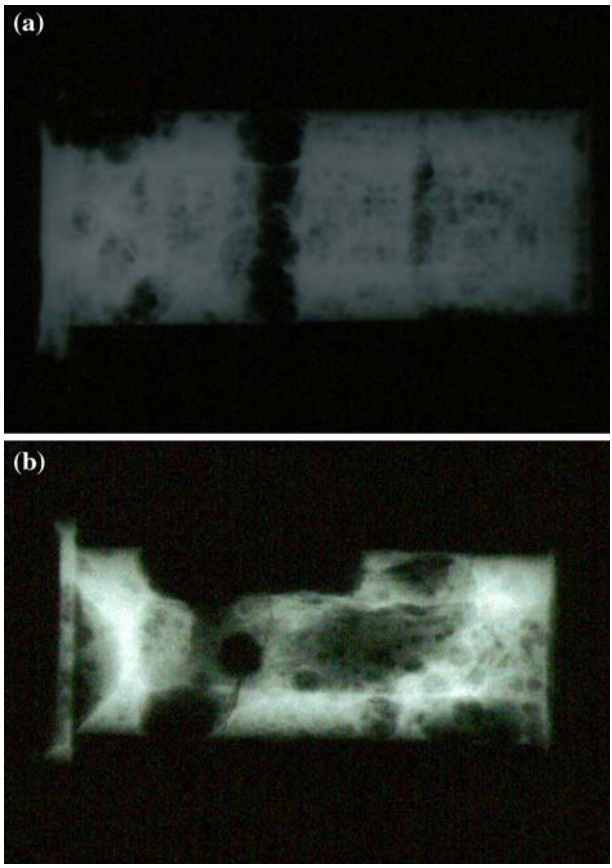

Fig. 3 X-ray transmission photo to check filling: (**a**) with C/C-sheet absorber and (**b**) without C/C-sheet absorber

of approximately 2 K. The measurement setup is described in [4]. The melting and freezing were realized by controlling the furnace temperature setting at a constant temperature offset ΔT above or below the equilibrium temperature.

4.2 Effect of Ingot Porosity

In Fig. 4a, the peritectic melting plateaux are compared for the 6SS-1 (porous ingot) and 6SS-2 (non-porous ingot) cells. The preceding freezing and the melting occurred with ΔT equal to -10 K and +20 K, respectively. As will be detailed in [4], the plateau durations are not always reproducible, even for the same melting conditions, for this fixed point. However, the plateau durations are similar, which is surprising if one considers the fact that the mass of the metal contained in 6SS-1 (porous) is 60% of that in 6SS-2 (non-porous).

In Fig. 4b, the eutectic melting plateaux of the same two cells are compared. Clearly, 6SS-1 shows shorter and weaker plateaux.

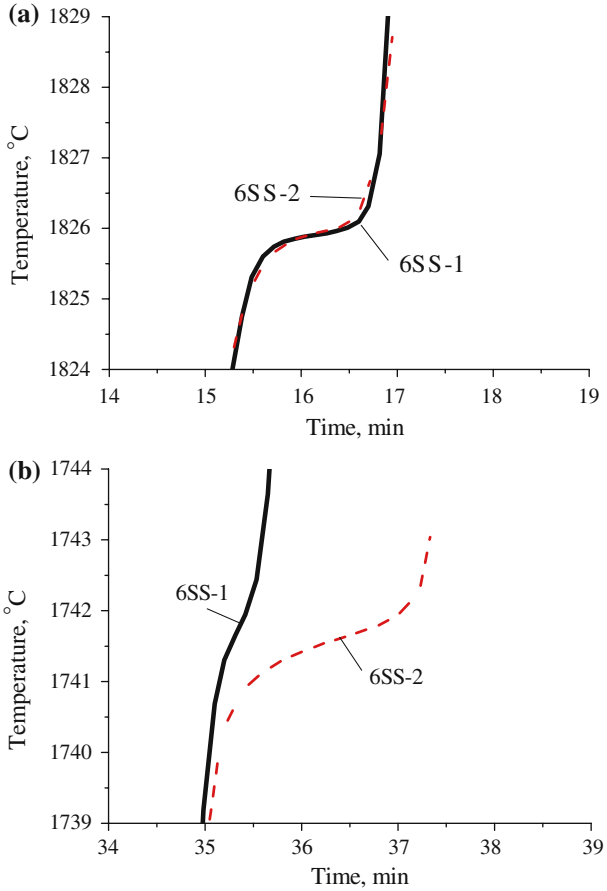

Fig. 4 Melting plateaux comparison between porous (6SS-1) and non-porous (6SS-2) ingot cells; measurement by LP-3 80-40 radiation thermometer: (**a**) peritectic and (**b**) eutectic

4.3 Comparison of Non-porous Cells with and without C/C-Sheet Absorber

In Fig. 5, the peritectic plateaux for 6ST-3 and 6SS-6 are compared. Note that the radiation thermometers are different: the difference in temperature when compared to Fig. 4a can be attributed to this. The plateau for 6ST-3 (with C/C-sheet absorber) has a slightly smaller melting range, and a sharper run-off at the plateau end, possibly relating to the more uniform ingot produced by using the C/C-sheet wick method. It is clear that this method should be followed when filling Cr_3C_2-C cells.

5 Microstructure Analysis

The behavior of eutectic fixed points is known to be strongly related to the microstructure being formed or dissolved, especially for the freeze, but in some cases for

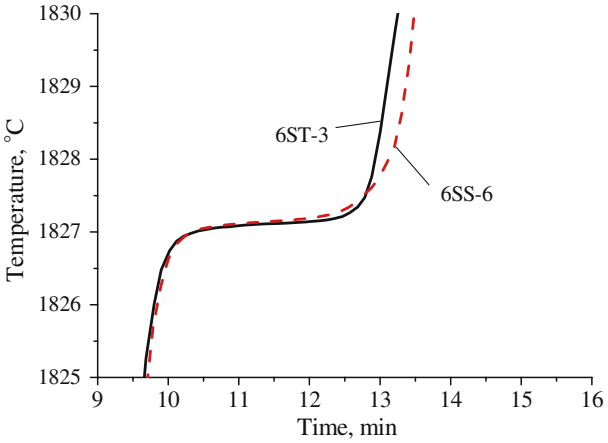

Fig. 5 Peritectic melting plateau comparison between cells with (6ST-3) and without (6SS-6) C/C-sheet absorber; measurement by LP-3 80-38 radiation thermometer

the melt as well [10–12]. Therefore, it is of interest to observe the structures formed by a peritectic reaction, and to consider the effect they may have on the melting or freezing temperature.

Unlike the M(C)-C eutectics, which have two distinct phases of graphite and metal that are identifiable upon microscope observation, the MC-C peritectics are composed of carbide phases that cannot be distinguished easily by the morphology of the cross section. To be more precise, in the case of the chromium-carbon system, one has to identify the graphite phase, the Cr_3C_2 phase formed on peritectic freezing, through the reaction $<C+(\text{Liquid solution of Cr and C}) \rightarrow Cr_3C_2>$, and the structure consisting of a mixture of Cr_3C_2 and Cr_7C_3 phases formed on eutectic freezing, through the reaction $<(\text{Liquid solution of Cr and C}) \rightarrow Cr_7C_3 + Cr_3C_2>$. The two carbide phases are indistinguishable by microscope observation.

Therefore, the cross sections of Cr_3C_2-C peritectic samples were analyzed by means of electron-probe microanalysis (EPMA) and back-scattered electron imaging (BSE). The EPMA can give two-dimensional scanned mapping of the concentration of selected elements. BSE maps the distribution of elements by taking advantage of the dependence of electron reflectance on the average atomic number. In Fig. 6, EPMA mapping of a non-porous ingot is shown of an area roughly $1.2\,\text{mm} \times 0.9\,\text{mm}$, at the border of the ingot in contact with the graphite crucible wall. Figure 6a shows the mapping of carbon, while Fig. 6b shows the mapping of chromium. The two are seen to be complementary. In Fig. 6c, mapping by means of BSE is shown. All three mappings are seen to be identical in structure.

For the EPMA mappings, the color scale, related to the concentration of the selected material, is shown on the right. The image shows the graphite crucible wall at the bottom (white in Fig. 6a and black in 6b), surrounded by carbon-rich domains (green in Fig. 6a and green to yellow in 6b). In the carbon-rich domains one can see embedded areas of graphite. Around the carbon-rich domain and detached from the graphite, the chromium-rich domain (blue in Fig. 6a and yellow to red in 6b) is found. The carbon-rich domain is considered to be the solid Cr_3C_2 formed by peritectic reaction.

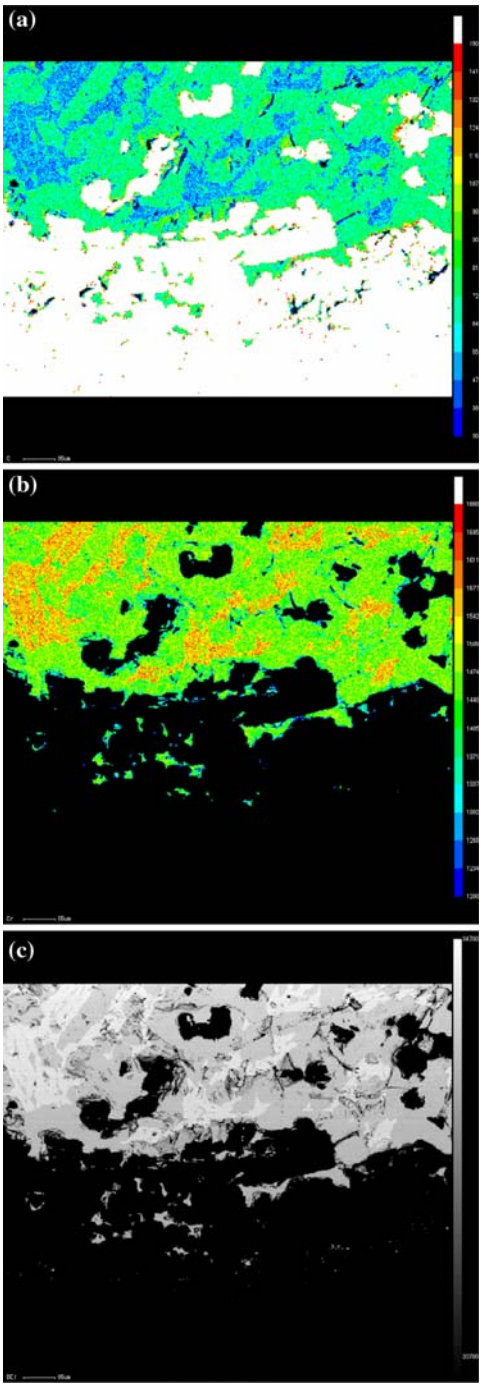

Fig. 6 EPMA and BSE mapping of non-porous ingot at crucible boundary: (**a**) EPMA for C, (**b**) EPMA for Cr, and (**c**) BSE

The chromium-rich domain is thought to be the part that remained liquid after the peritectic reaction, which subsequently froze in the eutectic reaction with further cooling, forming a eutectic mixture of Cr_7C_3 and Cr_3C_2. The spatial resolution of the imaging does not allow us to distinguish the fine eutectic structure, and we see a domain with a high average concentration of chromium.

In Fig. 7, EPMA mapping of the carbon is shown for the same non-porous ingot, and for a porous ingot. Both represent areas detached from the crucible wall of the same size as in Fig. 6. In contrast to what is observed in Fig. 6a, in the non-porous ingot (Fig. 7a) no graphite areas are observed, and the overall area of the carbon-rich domain (green) has decreased. For the porous ingot (Fig. 7b), pores (black) as well as graphite particles are seen. The overall area of the carbon-rich domain has increased when compared to Fig. 7a (non-porous ingot).

6 Discussion

When associating the measured plateaux with the microstructures observed, the ratio of the duration of the peritectic and eutectic plateaux appear to be related to the ratio of the overall areas of the carbon-rich and chromium-rich domains: the larger the carbon-rich domain, the longer the peritectic plateau. Therefore, the quality of the peritectic plateau should depend on the area and distribution of the chromium-rich domain.

The experimental evidence given above suggests that the graphite crucible plays a unique role in the MC-C peritectic reaction. During the MC-C peritectic freezing, the liquid reacts with carbon from the graphite to form the carbide. Therefore, the reaction should terminate as soon as all graphite has reacted. However, this can never happen in the current case: there is effectively an infinite supply of carbon from the graphite crucible, and therefore, in principle, the reaction can only terminate when all liquid has solidified. Carbon is supplied by diffusion through the solid carbide layer; its diffusion rate restricts the progress of the peritectic reaction. As shown in [4], the reaction continues even though the plateau indicates that freezing has finished. This argument is supported by the microstructure observation that any graphite surface, including the crucible wall, is surrounded by a carbon-rich layer, and that the carbon-rich domains are more abundant near the crucible surface.

The large surface area of the graphite crucible leads to an abundance of carbon-rich domains, which enables an extended peritectic plateau duration. Although non-uniformly distributed, the peritectic carbon-rich domain can always be found to surround the cavity.

The porous ingot has a larger surface area of graphite due to the embedded graphite flakes, with larger peritectic carbon-rich domains as observed in the microstructure, and this corresponds to the observed extended peritectic plateau and shorter eutectic plateau.

7 Summary

The MC-C peritectic fixed points were investigated with respect to their differences from the M(C)-C eutectic fixed points, by experiments based on the Cr_3C_2-C peritectic

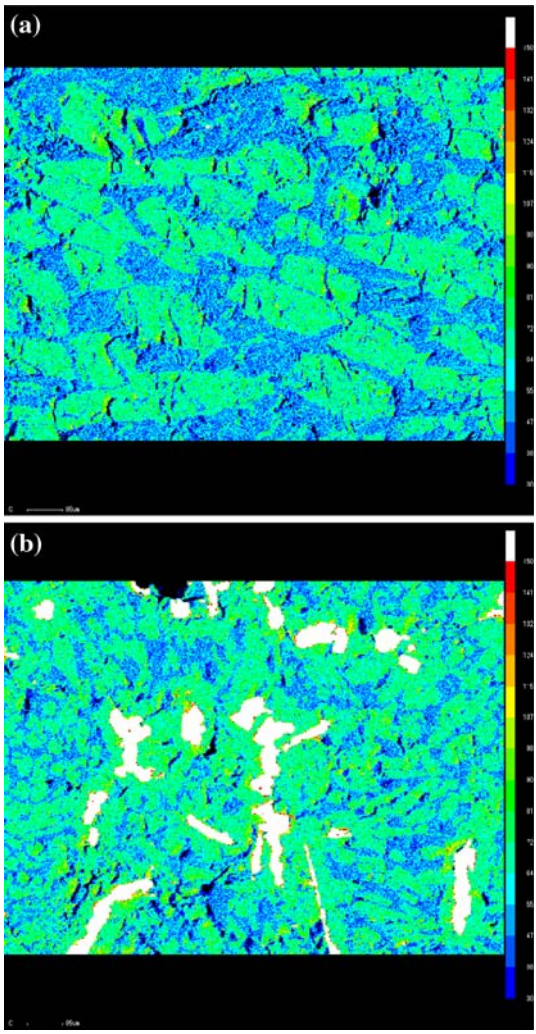

Fig. 7 EPMA mapping of C concentration of areas detached from the crucible: (**a**) non-porous ingot and (**b**) porous ingot

point. A difference in behavior in the molten state due to the low surface energy of the molten metal necessitated a new filling procedure utilizing a C/C-sheet absorber, which was shown to be capable of forming a void-free ingot. Microstructure analysis in conjunction with fixed-point plateau observation revealed the critical role that the graphite crucible surface plays in extending the plateau. The current study provides insight as to how to profit from the salient features of the fixed points [4]. Further study is envisaged to better understand the peritectic melting phenomena, including the effect of impurities.

Acknowledgments Prof. Seiji Miura of Hokkaido Univ. is acknowledged for his helpful advice on microstructure analysis. P. Bloembergen of the NMIJ is thanked for his critical comments.

References

1. G. Machin, P. Bloembergen, J. Hartmann, M. Sadli, Y. Yamada, in *Proc. TEMPMEKO 2007*, Int. J. Thermophys (in press)
2. E.R. Woolliams, G. Machin, D.H. Lowe, R. Winkler, *Metrologia* **43**, R11 (2006)
3. Y. Yamada, Y. Wang, N. Sasajima, *Metrologia* **43**, L23 (2006)
4. W. Zheng, Y. Yamada, Y. Wang, in *Proc. TEMPMEKO 2007*, to be published in Int. J. Thermophys.
5. N. Sasajima, Y. Yamada, Y. Wang, in *Proc. TEMPMEKO 2007*, to be published in Int. J. Thermophys.
6. H. Okamoto, ed., *Desk Handbook Phase Diagrams for Binary Alloys* (ASM Int., Materials Park, OH, 2000)
7. K. Anhalt, Y. Wang, Y. Yamada, J. Hartmann, in *Proc. TEMPMEKO 2007*, to be published in Int. J. Thermophys.
8. D. Lowe, Y. Yamada, *Metrologia* **43**, S135 (2006)
9. Y. Yamada, B. Khlevnoy, Y. Wang, T. Wang, K. Anhalt, *Metrologia* **43**, S140 (2006)
10. N. Sasajima, Y. Yamada, Y. Wang, P. Bloembergen, T. Wang, J. Le Coze, *J. Alloy. Compd*. (in press)
11. P. Bloembergen, Y. Yamada, N. Sasajima, Y. Wang, T. Wang, *Metrologia* **44**, 279 (2007)
12. D. Lowe, K. Mingard, Z. Malik, P. Quested, in *Proc. TEMPMEKO 2007*, to be published in Int. J. Thermophys.